CORROSION INHIBITIVE PROPERTIES OF THE HYDROPHOBIC COATINGS ON PEO-PRETREATED ALUMINUM ALLOY

Sergey L. Sinebryukhov, Sergey V. Gnedenkov, Vladimir S. Egorkin, Igor E. Vyaliy

Institute of Chemistry, Far Eastern Branch, Russian Academy of Sciences, 159, Prosp. 100-letya Vladivostoka, Vladivostok, 690022, Russia, sls@ich.dvo.ru

Abstract: The plasma electrolytic oxidation (PEO) was used to form on the AMg3 aluminum alloy the high adhesive oxide coating as a base barrier layer with necessary microrelief. Morphology, composition, and barrier properties of hydrophobic and superhydrophobic coatings on the surface PEO pretreated aluminum alloy have been investigated. Results of the study of such layers, which underwent PEO and additional treatment under UV-radiation in the presence of ozone plasma with subsequent deposition of the hydrophobic agent have been described. The formed composite layers were found to be characterized with hydrophobicity and high barrier properties. Coatings formed by deposition of the hydrophobic agent dispersion containing SiO_2 nanoparticles on the PEO-layer are characterized by highest contact angle and inhibitive properties.

It was established that transition from hydrophobic to superhydrophobic properties was provided by formation of the nanoparticles aggregates on the surface, thus realizing a multimodal roughness. Electrochemical measurements revealed high barrier properties provided by PEO-layer and the nanocomposite superhydrophobic surface formed by deposition from nanoparticle dispersion onto base PEO-coating during the 48 h of exposure to aggressive media. It was established that low surface energy and specific multimodal morphology of the surface ensure the superhydropobic properties of the composite layer.

Keywords: plasma electrolytic oxidation, wettability, hydrophobicity, contact angle, electrochemical impedance spectroscopy

INTRODUCTION

Search for efficient methods of metals and alloys protection against corrosion is one of the most important priority topics of the advanced material science development.

The range of practical applications of metals and alloys could be expanded significantly using plasma electrolytic oxidation (PEO) to form the protective oxide layer on the surface of titanium (1), magnesium (2, 3), aluminum (4, 5), and even steel (6, 7).

Formation of hydrophobic (HP) and superhydrophobic (SHP) coatings on magnesium (8, 9), titanium (10), steel (6, 11), aluminum (12, 13), and other metals and alloys and study of their inhibitive properties comprise important stages of the development of anticorrosion coatings characterized by reliable protective properties not only under atmospheric conditions, but also in aggressive media.

The inhibitive effect of such type of coatings is determined by the combined contribution of many factors (6). The main factors are the barrier properties and chemical composition of the base PEO-layer, contact angle (CA) values, morphological features of coating texture, the adhesion of water repelling top-layer to

a surface, and the interaction between the electrolyte and the base metal and between the electrolyte and components of coating.
The reported results indicate that application of the SHP-layers on aluminum alloys usually leads to reduction of corrosion currents density by 2–3 orders of magnitude in comparison with the bare substrate (12, 13). In view of this, the search for the methods to further increase the barrier properties is still an urgent topic.
The hydrophobic agent that was used in this paper performs two functions. First, it reduces the free surface energy of the material. Second, it has three reactive terminal groups, $–Si(OCH_3)_3–$, thus providing a chemical bond between the nanoparticles in the aggregates and between the nanoparticles and the PEO-layer (6, 8).
The objective of the present study was to provide a method of the hydrophobic layers formation on the PEO-pretreated aluminum alloy by means of the deposition of the hydrophobic agent from solution in decane and to investigate barrier properties of the formed layers by electrochemical impedance spectroscopy (EIS).

EXPERIMENTAL

The wrought aluminum alloy AMg3 (analog of 5754 aluminum alloy) belonging to Al–Mg–Mn–Si system (wt. %: Mg 3.75; Si 0.78; Mn 0.38; Fe 0.43; Zn 0.10; Cu 0.10; Ti 0.10; Cr 0.05; Al 94.31) was used as a substrate. Rectangular samples of a size of 40 mm × 15 mm × 1.5 mm were ground using abrasive SiC paper up to 1200 grit. PEO was carried out in the electrolyte containing 20 g/l $C_4H_4O_6K_2 \cdot 0.5H_2O$ and 1.5 g/l NaF. Samples were treated in the unipolar galvanostatic mode with $j = 1.45$ A/cm^2 for 150 s. The polarizing pulses frequency was equal to 300 Hz (pulse duration 3.3 ms, no pauses). The duty cycle was equal to 100 %.
In order to increase the number of chemisorption-active centres, the samples after plasma electrolytic oxidation were placed into a UV Cleaner chamber for 50 min, where ozone plasma was created under UV radiation.
The hydrophobic (PEO + MAF) coating was formed as the result of the deposition of the hydrophobic layer from the solution of the methoxy-{3-((2,2,3,3,4,4,5,5,6,6,7,7,8,8,8-pentadecafluoroctyl)oxy)propyl}-silane (MAF) in anhydrous decane atop the PEO-coating treated with UV-radiation.
The superhydrophobic composite coating (PEO + MAF + SiO_2) was formed at ambient conditions atop of PEO-coating treated with UV-radiation by the deposition from the wetting film of 3 % SiO_2 nanoparticle suspension in decane.
SEM-images of the samples surface and the data on their elemental composition were obtained with a Hitachi S5500 scanning electron microscope.
Electrochemical properties of the formed coatings were studied on a Solartron ModuLAB equipped with femtoammeter. Measurements were carried out in a three-electrode cell with 3 % NaCl aqueous solution as an electrolyte. The exposed sample surface area was equal to 1 cm^2.
The characterization of wettability of coatings was based on the static contact angle (CA) and rolling angle (RA) measurements. To measure the CAs, the method of digital image processing of a sessile drop of the testing liquid on the investigated surface was used. Testing liquid was 3 % solution (pH = 7) of chemically pure NaCl in 18 MOhm·cm deionized water. A Krűss DSA100 device was used to perform measurements of the contact and rolling angles and to obtain optical images of the sessile drops.

RESULTS AND DISCUSSION

Effect of Treatment Conditions on Morphology, Composition, and Wetting Parameters of the Coatings

Application of the short and intensive formation PEO mode, involving the current with high peak values, ensured formation of the oxide layer, possessing the desired type of morphology. SEM-images in Fig. 1 represent the surface morphology of the formed coatings and give the insight to their structure through the cross-sections. PEO-layers are composed of microtubes having a 200–300 μm diameter and grown normally to the substrate. Such type of surface structure is typical for the layers formed in tartrate electrolytes at early stages of the PEO-process (15).

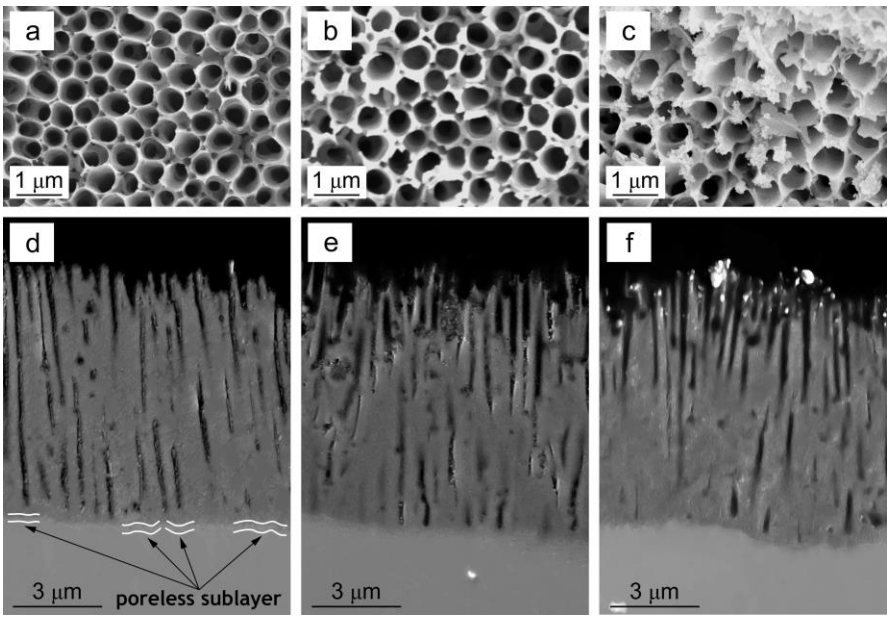

Fig. **1**. SEM-images of the surface (a, b, c) and cross-sections (d, e, f) for coatings: PEO (a, d), PEO + MAF (b, e), and PEO + MAF + SiO_2 (c, f).

Obviously, the MAF-treatment cannot cause visible changes in morphology because the thickness of hydrophobic agent from solution is about one monolayer (6). The process of self-organization of nanoparticles in a wetting film of the dispersion, containing silica nanoparticles, hydrophobic agent, and low-volatile dehydrated dispersion medium results in precipitation and aggregation of the SiO_2 nanoparticles predominantly in the junction points of the microtube walls, forming multimodal hierarchical roughness (Fig.1 c, f). Results of the analysis of the chemical composition are presented in Table 1.

Table **1**. Composition of the coatings

Sample	Elemental composition (wt. %)					
	C	O	F	Al	Si	K
PEO	8.3±1.7	48.9±0.9	3.4±0.7	38.4±0.3	0.3±0.1	0.7±0.1
PEO+MAF	14.2±3.6	29.7±1.6	13.4±1.1	39.6±0.5	2.5±0.2	0.6±0.1
PEO+MAF+SiO_2	29.7±1.6	17.8±0.9	13.4±0.7	28.4±0.6	10.7±0.4	–

Wetting measurements demonstrated that the initial PEO-coatings are hydrophilic, and show the contact angle of (35.9 ± 2.9)º . The HP-layer on the PEO-coating treated with ozone plasma formed by deposition of MAF monolayer showed the contact angle (160.1 ± 6.9)º and rolling angle (17.5 ± 8.8)º.
It should be emphasized that rolling angle values for this type of coating are higher than those appropriate for superhydrophobic materials. PEO + MAF + SiO_2 coating demonstrates higher values of the contact angle (164.5 ± 3.3)º and lower values of the rolling angle (8.2 ± 2.7)º. Taking into account that wetting properties of the hydrophobic layers being in contact with water or brine solution might significantly change with time (16), a prolonged measurement of the CAs was performed. The conducted study revealed (Fig. 2) that the layer formed with nanoparticles is characterized by stable CA values of the brine solution drop being settled onto the coating.

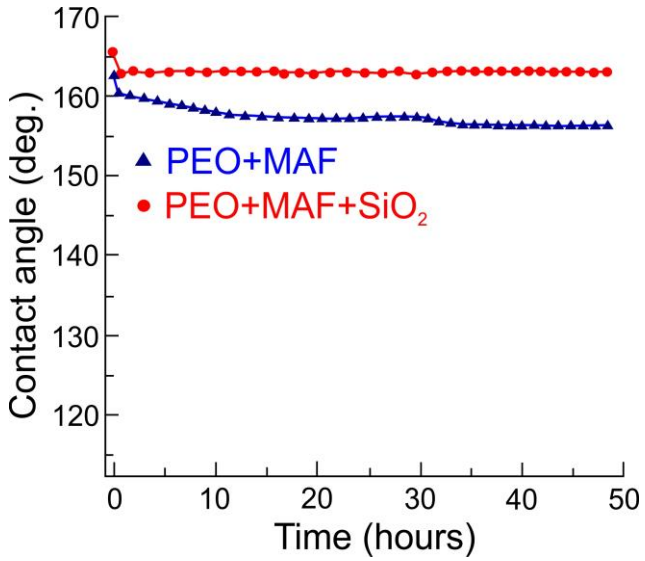

Fig. **2**. The evolution of the contact angle with time after deposition of the drop of 3 % NaCl aqueous solution on samples.

Results of the OCP Monitoring and Potentiodynamic Polarization Tests

OCP evolution for studied samples as a function of immersion time is presented in Fig. 3. From the shape of the curves, one can conclude that one hour of immersion is enough time for the potential stabilization during initial period of the samples exposition to the solution. Except the PEO + MAF, all the investigated samples demonstrate stable values of the OCP. In case of the uncoated sample, this is due to the formation of the film of corrosion products on the surface and the pits sites. The PEO-coating also demonstrates almost constant values with slight increase after the 20 h of immersion. The coating formed by the deposition of the hydrophobic layer onto the PEO-coating exhibits quite different behavior, showing the initial rise of the OCP from –0.6 V to –0.45 V in the range 5–15 h with subsequent decrease and stabilization at –0.65 V after 35 h of exposure.

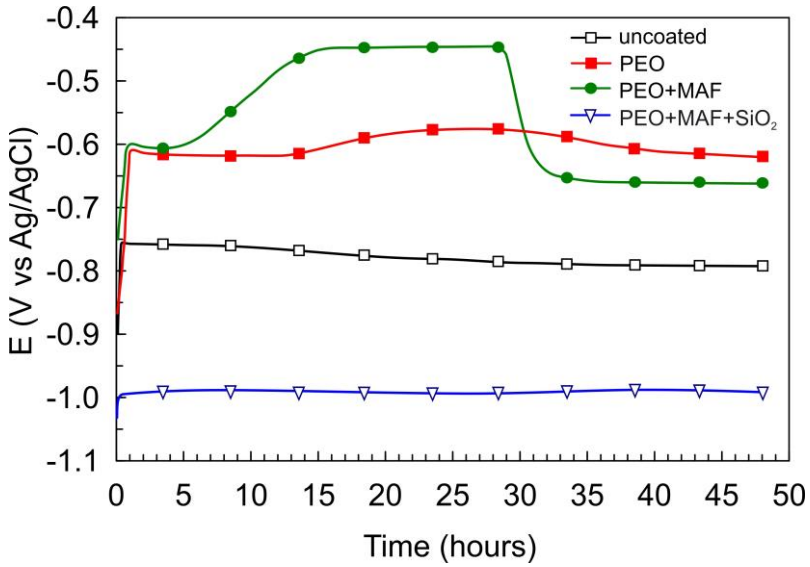

Fig. **3**. OCP evolution during the exposure of the samples to 3 % NaCl for 48 h.

Polarization curves for the aluminum alloy samples without coating, with PEO-coating, with HP-coating, and with SHP-coating are shown in Fig. 4. The obtained data demonstrate that the barrier properties and the reliability of inhibition are significantly increased with the nanoparticles embedding. The value of the corrosion current density calculated from the experimental data for SHP-coating is equal to 4.6×10^{-14} A/cm^2, which is more than 7 orders of magnitude lower than one for the sample without coating (6.1×10^{-7} A/cm^2), lower than for the HP-coating by two orders of magnitude (4.8×10^{-12} A/cm^2), and practically by 4 orders of magnitude lower than for the PEO-layer (3.5×10^{-10} A/cm^2) (Table 2).

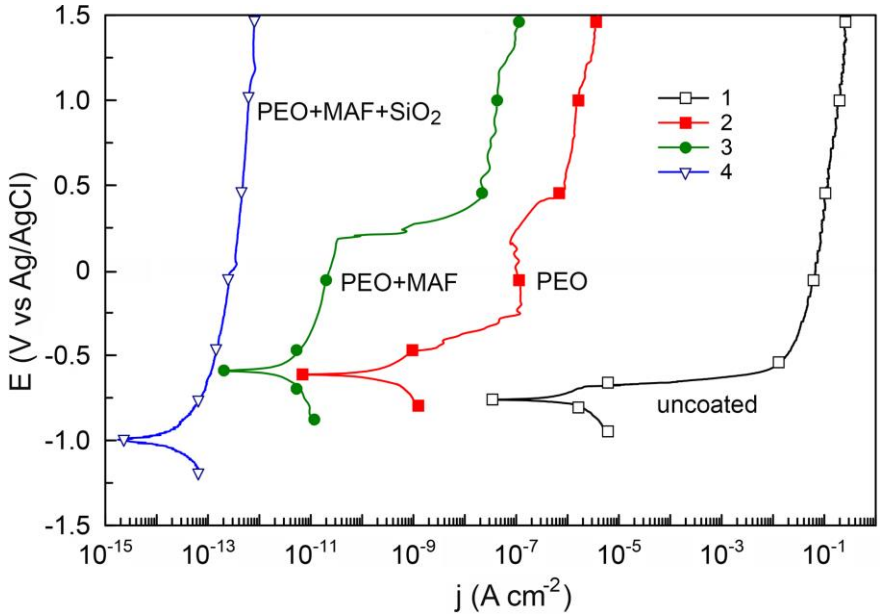

Fig.**4**. Polarization curves obtained in 3 % NaCl solution for the aluminum alloy samples with different surface layers: 2 – PEO, 3 – HP-coating formed by deposition of hydrophobic agent monolayer atop the PEO-coating (PEO + MAF), 4 – nanocomposite SHP-coating formed by aggregation of silica nanoparticles (PEO + MAF + SiO_2). Curve 1 – for the uncoated sample provided for comparison.

Table **2**. Electrochemical parameters of the aluminum alloy samples

Sample	E_C (V vs Ag/AgCl)	B (mV)	j_C (A cm^{-2})	R_p (Ω cm^2)
Uncoated	–0.76	17.5	6.1×10^{-7}	2.9×10^{4}
PEO	–0.61	58.4	3.5×10^{-10}	1.7×10^{8}
PEO + MAF	–0.60	110.0	4.8×10^{-12}	2.2×10^{10}
PEO + MAF + SiO_2	–0.99	145.6	4.6×10^{-14}	3.1×10^{12}

Analysis of the experimental results presented in Table 2 corroborated the increase of the protective properties of the samples with SHP and HP-coatings in comparison with the uncoated sample and the base PEO-layer. The specimen with the nanocomposite superhydrophobic coating formed by aggregation of silica nanoparticles is characterized with higher value of the polarization resistance ($R_P = 3.1\times10^{12}$ Ω cm^2) as compared to the samples without coating ($R_P = 2.9\times10^{4}$ Ω cm^2) and with PEO-coating ($R_P = 1.7\times10^{8}$ Ω cm^2).

Electrochemical Impedance Spectroscopy Studies

The graphs of the dependence of the impedance modulus on frequency (Fig. 5 a) corroborate the conclusions based on the analysis of polarization curves. The values of the impedance modulus measured at low frequency ($|Z|_{f = 0.01\ Hz}$) for the SHP sample are 1.1×10^{11} Ω cm^2, that is by 12-fold higher than those for the HP-coating (9.2×10^{9} Ω cm^2) and more than by six orders of magnitude higher than that of the bare substrate (2.9×10^{4} Ω cm^2) itself (Table 3).

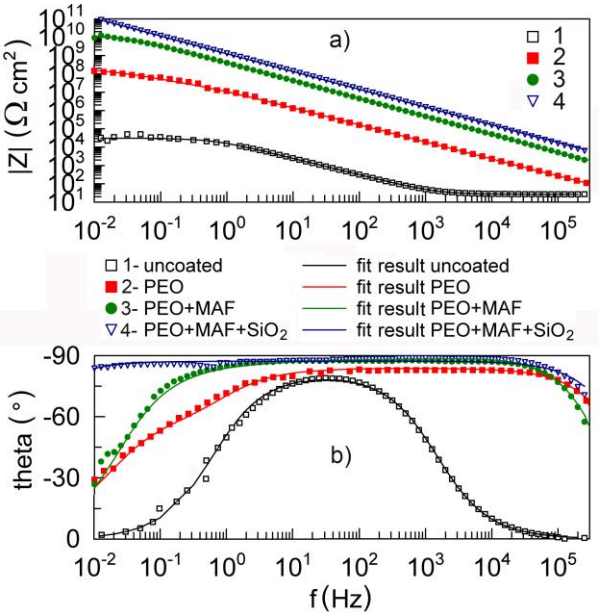

Fig. **5**. Bode plots (a) impedance modulus |Z| and (b) phase angle theta vs. frequency f) obtained in 3 % NaCl for the investigated samples: 2 – PEO, 3 – HP-coating formed by deposition of hydrophobic agent monolayer atop the PEO-coating (PEO + MAF), 4 – nanocomposite SHP-coating formed by aggregation of silica nanoparticles (PEO + MAF + SiO_2), obtained in 3 % NaCl solution. Curve 1 – for the uncoated sample provided for comparison. Symbols are experimental data, solid lines are fitting curves.

Electrochemical impedance spectra shown in Fig. 5 as Bode plots contain experimental data (scatter plots marked by symbols) and theoretical fitting curves (solid lines), which simulate the experimental results by means of equivalent electrical circuits (EEC) (Fig. 6). Results of the fitting of the experimental EIS-data (Fig. 5) to appropriative EEC and impedance modulus values, obtained at 0.01 Hz, are presented in Table 3. Electrochemical simulation of the processes of charge transfer at the coating/electrolyte interface was performed on the basis of a systematic approach, in which the object under study is described by the equivalent electrical circuit including elements characterizing the electrode/electrolyte interface.

Table **3**. Calculated parameters of the equivalent electrical circuit elements for the aluminum alloy samples. These parameters were used for plot of fitting curves (solid lines in Fig. 5).

Sample	CPE_1		R_1 (Ω cm^2)	CPE_2		R_2 (Ω cm^2)	$\lvert Z\rvert_{f=0.01}$ (Ω cm^2)
	Q_1 (S cm^{-2} c^n)	n		Q_2 (S cm^{-2} c^n)	n		
Uncoated				0.9×10^{-6}	0.91	3.1×10^{4}	2.9×10^{4}
PEO	1.5×10^{-8}	0.93	3.5×10^{7}	1.7×10^{-8}	0.70	1.7×10^{8}	1.4×10^{8}
PEO + MAF	3.4×10^{-10}	0.99	5.7×10^{7}	1.2×10^{-10}	0.73	1.4×10^{10}	9.2×10^{9}
PEO + MAF + SiO_2	1.3×10^{-10}	0.98	9.7×10^{11}	7.3×10^{-11}	0.97	2.9×10^{12}	1.1×10^{11}

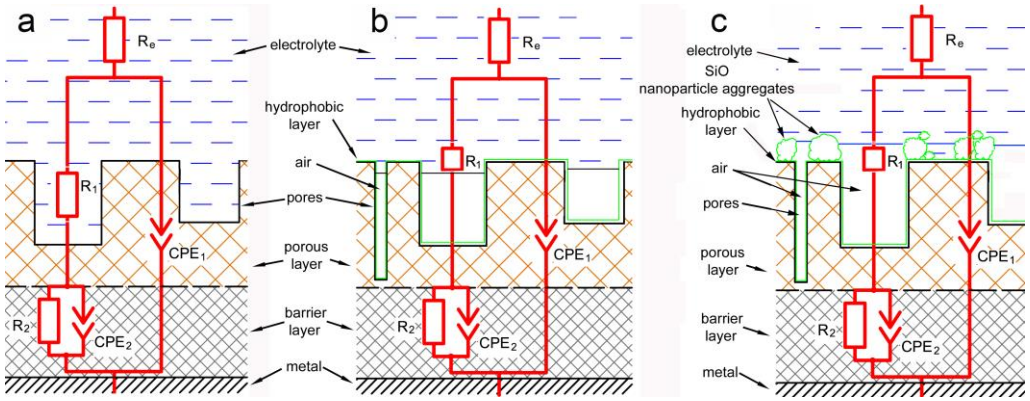

Fig. **6**. Graphical representation of electrolyte/coating interface and equivalent electrical circuits used for fitting the experimental impedance data for aluminum alloy samples: a – PEO, b – PEO + MAF, and c – PEO + MAF + SiO_2.

The electrode/electrolyte interface for the uncoated sample is well described by EEC with one *R-CPE* circuit, characterizing the behavior of the natural oxide film. Samples with PEO-coating, HP and SHP-layers were described by the EECs in Fig. 6 b, c, which also depict the differences in physical meaning of the EECs for the different coatings.

For the uncoated sample $|Z|_{f=0.01}$ is equal to 2.9×10^4 Ω cm^2. The dependency of the phase angle on the frequency contains the one time constant at frequencies 10^4–1 Hz (Fig. 5 b) caused by the presence of the natural oxide film on alloy's surface. In case of the uncoated alloy, *R* – is the charge transfer resistance, and *CPE* – capacitance of the natural oxide film.

In the spectrum of the sample with the PEO-coating two bends are observed in a broad frequency range from 10^6 to 0.01 Hz (Fig. 5 b). The values of the phase angle

(*theta*) are close to –90º, which indicates to the capacitive character of the investigated interface. The impedance fitting practice and the PEO-layer structure data confirm the presence of two time constants (two bends on the dependency of the phase angle on the frequency) represented porous and poreless parts of the PEO-layer. CPE_1 — the geometric capacity of the PEO-coating. The element R_1 parallel to CPE_1 is responsible for electrical resistance to the ionic current in pores. The parallel chain CPE_2–R_2 is used to describe the process of charge transfer in the coating nonporous internal sublayer. The resistance of this coating is equal to $|Z|_{f = 0.01} = 1.4\times10^8$ Ω cm^2 (Table 3), which characterizes the base PEO-layer as that of the barrier type having high inhibitive properties.

The hydrophobic coating on the PEO-layer (Fig. 5, curve 3) and the SHP-coating (Fig.5, curve 4) have one apparent bend on the phase angle versus frequency dependence. They also can be fitted with the one *R-CPE* circuit with the lesser values of chi-squared than for two *R-CPE* circuit EEC. The choice of the EEC with two *R-CPE* chains was determined by the physical meaning of the constituent elements. For the HP-coating, CPE_1 — models the geometric capacitance of the composite layer as a whole. The element R_1 parallel to CPE_1 is responsible for electrical resistance to the ionic current in pores and air trapped in pores. The parallel chain CPE_2–R_2 is used to describe the process of charge transfer in the coating poreless internal sublayer including the layer of the hydrophobic agent on the pore walls. The value $|Z|_{f = 0.01}$ for HP is equal to 9.2×10^9 Ω cm^2 (Table 3). In case of the SHP-coating, CPE_1 also includes the nanoparticles aggregates in the whole thickness. Treatment of the PEO-coating by SiO_2 dispersion leads to formation of the coating with the high impedance modulus at lowest frequency ($|Z|_{f = 0.01} = 1.1\times10^{11}$ Ω cm^2). Comparison of the Q_1 values for the HP-coating (3.4×10^{-10} S cm^{-2} c^n) and the SHP-coating (1.3×10^{-10} S cm^{-2} c^n) (Table 3) using the flat capacitor equation, leads to the conclusion that SHP-coating is much thicker than the HP-coating, owing to nanoparticles aggregates, which entrap and form thicker air layers. The values of R_2 enable one to assume that not only the hydrophobic agent, but also nanoparticles might precipitate at the bottom of the pores, which result in the increase of resistance of the barrier layer in the row: PEO (1.7×10^8 Ω cm^2), HP (1.4×10^{10} Ω cm^2), SHP (2.9×10^{12} Ω cm^2) (Table 3).

The evolution of the impedance modulus values measured at 0.01 Hz over time during exposure of the samples to 3 % NaCl aqueous solution for two days (Fig. 7) reveals that there are significant differences in the mechanism oft the samples interaction with the aggressive media. The measurements confirm a high stability of the SHP-layer and supplement the data derived from wettability and OCP experiments. For the uncoated alloy, the decrease of impedance values during first 12 h of exposition is associated with the initiation and development of pits in the passive layer of natural oxide being in contact with chloride-containing electrolyte. The subsequent increase of impedance values is related to precipitation of the film of corrosion products thus inhibiting the further corrosion development. The shape of the curve of impedance modulus values for the PEO-coating resembles a mirror reflection of the OCP-curve with decrease of impedance corresponding when the OCP values increase.

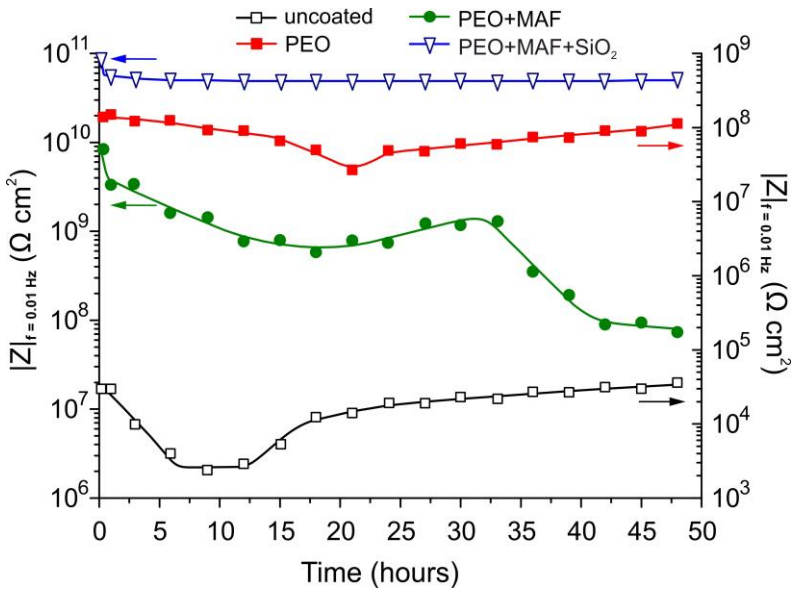

Fig. 7. The evolution of the impedance modulus values measured at 0.01 Hz with time during exposure of the samples to 3% NaCl solution for 48 h.

CONCLUSIONS

As a result of performed studies, the morphological structure and elemental composition of the formed layers have been reported. It was established that transition from hydrophobic to superhydrophobic properties was provided by formation of the nanoparticles aggregates on the surface, thus realizing a multimodal roughness.

Electrochemical measurements revealed a high level of barrier properties provided by PEO-layer and the nanocomposite superhydrophobic surface formed by deposition from nanoparticle dispersion onto base PEO-coating for the initial period of contact with the aggressive media and during the 48 h of exposure. The impedance modulus value of the SHP-coating is maximal among the investigated layers and is equal to $|Z|_{f=0.01} = 1.1\times10^{11}$ Ω cm^2. It was established that low surface energy and specific multimodal morphology of the surface, providing formation of the three-phase interface (coating/gas/electrolyte), ensure the superhydropobic properties of the composite layer.

The coatings might be considered as promising to be used for corrosion protection; however, it is necessary to conduct further studies on long-term resistance to aggressive media, UV radiation, mechanical damage, and other effects in accordance with the relevant standards.

ACKNOWLEDGEMENTS

This work was supported by the Russian Science Foundation (№ 14-33-00009).
Authors thank Prof. L.B. Boynovich and Prof. A.M. Emelyanenko (IPCE RAS, Moscow) for participation in the development of hydrophobic coatings and wetting measurements.

REFERENCES

1. Mirelman L, Curran J, Clyne T: 'The production of anatase-rich photoactive coatings by plasma electrolytic oxidation'. Surf. Coat. Technol. 2012 (207) 66–71.

2. Snizhko L, Yerokhin A, Gurevina N, Misnyankin D, Ciba A, Matthews A: 'Voltastatic studies of magnesium anodising in alkaline solutions'. Surf. Coat. Technol. 2010 (205) 1527–1531.
3. Sinebryukhov S, Sidorova M, Egorkin V, Nedozorov P, Ustinov A, Volkova E, Gnedenkov S: 'Protective oxide coatings on Mg–Mn–Ce, Mg–Zn–Zr, Mg–Al–Zn–Mn, Mg–Zn–Zr–Y, and Mg–Zr–Nd magnesium-based alloys'. Prot. Met. Phys. Chem. Surf. 2012 (48) 678–687.
4. Khan R, Yerokhin A, Li X, Dong H, Matthews A: 'Surface characterisation of DC plasma electrolytic oxidation treated 6082 aluminium alloy: Effect of current density and electrolyte concentration'. Surf. Coat. Technol. 2010 (205) 1679–1688.
5. Mohedano M, Matykina E, Arrabal R, Mingo B, Pardo A: 'PEO of pre-anodized Al-Si alloys: Corrosion properties and influence of sealings'. Appl. Surf. Sci. 2015 (346) 57–67.
6. Boinovich L, Gnedenkov S, Alpysbaeva D, Egorkin V, Emelyanenko A, Sinebryukhov S, Zaretskaya A: 'Anticorrosion performance of composite coatings on low-carbon steel containing highly- and superhydrophobic layers in combination with oxide sublayers'. Corros. Sci. 2012 (55) 238–245.
7. Malinovschi V, Marin A, Moga S, Negrea D: 'Preparation and characterization of anticorrosive layers deposited by micro-arc oxidation on low carbon steel'. Surf. Coat. Tech. 2014 (253) 194–198.
8. Gnedenkov S, Sinebryukhov S, Egorkin V, Mashtalyar D, Emelyanenko A, Boinovich L: 'Electrochemical properties of the superhydrophobic coatings on metals and alloys'. J. Taiwan Inst. Chem. E. 2014 (85) 3075–3080.
9. Liu Q, Chen D, Kang Z: 'One-Step Electrodeposition Process To Fabricate Corrosion-Resistant Superhydrophobic Surface on Magnesium Alloy'. ACS Appl. Mater. Interfaces 2015 (7) 1859–1867.
10. Gnedenkov S, Sinebryukhov S, Egorkin V, Mashtalyar D, Emel'yanenko A, Alpysbaeva D, Boinovich L: 'Features of the Occurrence of Electrochemical Processes in Contact of Sodium Chloride Solutions with the Surface of Superhydrophobic Coatings on Titanium'. Russ. J. Electrochem+. 2012 (48) 336–345.
11. Yu D, Tian J, Dai J, Wang X: 'Anticorrosion Behavior of Superhydrophobic Composite Coating on Carbon Steel in Seawater'. Corrosion 2014 (70) 329–336.
12. Lv D, Ou J, Xue M, Wang F: 'Stability and corrosion resistance of superhydrophobic surface on oxidized aluminum in NaCl aqueous solution'. Appl. Surf Sci. 2015 (333) 163–169.
13. Zhang F, Zhao, L Chen H, Xu S, Evans D, Duan X: 'Corrosion resistance of superhydrophobic layered double hydroxide films on aluminum'. Angew. Chem. Int. Ed. 2008 (47) 2466–2469.
14. ASTM G59–97(2009), Standard Test Method for Conducting Potentiodynamic Polarization Resistance Measurements, ASTM International, West Conshohocken, PA, 2009.
15. Gnedenkov S, Khrisanfova O, Zavidnaya A, Sinebrukhov S, Gordienko P, Iwatsubo S, Matsui A: 'Composition and adhesion of protective coatings on aluminium'. Surf. Coat. Technol. 2001 (145/1–3) 146–151.
16. Boinovich L, Emelyanenko A, Pashinin A: 'Analysis of Long-Term Durability of Superhydrophobic Properties under Continuous Contact with Water'. ACS Appl. Mater. Interfaces 2010 (2) 1754–1758.